



# CHORUS

This is the accepted manuscript made available via CHORUS. The article has been published as:

## Observation of Classical-Quantum Crossover of $1/f$ Flux Noise and Its Paramagnetic Temperature Dependence

C. M. Quintana *et al.*

Phys. Rev. Lett. **118**, 057702 — Published 31 January 2017

DOI: [10.1103/PhysRevLett.118.057702](https://doi.org/10.1103/PhysRevLett.118.057702)

# Observation of classical-quantum crossover of $1/f$ flux noise and its paramagnetic temperature dependence

C. M. Quintana,<sup>1</sup> Yu Chen,<sup>2</sup> D. Sank,<sup>2</sup> A. G. Petukhov,<sup>3</sup> T. C. White,<sup>2</sup> Dvir Kafri,<sup>4</sup> B. Chiaro,<sup>1</sup> A. Megrant,<sup>2</sup> R. Barends,<sup>2</sup> B. Campbell,<sup>1</sup> Z. Chen,<sup>1</sup> A. Dunsworth,<sup>1</sup> A. G. Fowler,<sup>2</sup> R. Graff,<sup>2</sup> E. Jeffrey,<sup>2</sup> J. Kelly,<sup>2</sup> E. Lucero,<sup>2</sup> J. Y. Mutus,<sup>2</sup> M. Neeley,<sup>2</sup> C. Neill,<sup>1</sup> P. J. J. O'Malley,<sup>1</sup> P. Roushan,<sup>2</sup> A. Shabani,<sup>4</sup> V. N. Smelyanskiy,<sup>4</sup> A. Vainsencher,<sup>2</sup> J. Wenner,<sup>1</sup> H. Neven,<sup>4</sup> and John M. Martinis<sup>1,2</sup>

<sup>1</sup>*Department of Physics, University of California, Santa Barbara, California 93106, USA*

<sup>2</sup>*Google Inc., Santa Barbara, California 93117, USA*

<sup>3</sup>*NASA Ames Research Center, Moffett Field, California 94035, USA*

<sup>4</sup>*Google Inc., Venice, CA 90291, USA*

(Dated: December 7, 2016)

By analyzing the dissipative dynamics of a tunable gap flux qubit, we extract both sides of its two-sided environmental flux noise spectral density over a range of frequencies around  $2k_B T/h \approx 1$  GHz, allowing for the observation of a classical-quantum crossover. Below the crossover point, the symmetric noise component follows a  $1/f$  power law that matches the magnitude of the  $1/f$  noise near 1 Hz. The antisymmetric component displays a  $1/T$  dependence below 100 mK, providing dynamical evidence for a paramagnetic environment. Extrapolating the two-sided spectrum predicts the linewidth and reorganization energy of incoherent resonant tunneling between flux qubit wells.

The ubiquity of low-frequency magnetic flux noise in superconducting circuits has been well-known for decades [1–8], making it perhaps surprising that its microscopic origin has yet to be determined. Understanding the origin of flux noise will be crucial to reduce it. For example, this would inform experiments attempting to modify the noise using surface treatments [9]. Flux noise causes parameter drift and loss of phase coherence, and its reduction is a key task for technologies based on flux-sensitive superconducting circuits. In quantum annealing, low-frequency noise limits the number of qubits that can coherently tunnel, and a dissipative environment can suppress incoherent quantum tunneling [10–14].

In the past decade, superconducting qubits have extended the measurement of flux noise to increasingly wider frequency ranges, showing a  $1/f^{\alpha(f)}$  power spectrum from  $f \approx 10^{-5}$  Hz to  $f \approx 1$  GHz with  $\alpha$  close to 1 at low temperatures [5, 15–21]. Although previous frequency-resolved measurements of this noise have used a variety of experimental methods, they have extracted only a single quantity, the symmetrized spectrum  $S_{\Phi}^+(f)$ , to describe the noise. However, as is well known, a quantum environment can generate different noise spectra at positive and negative frequencies,  $S_{\Phi}(-f) \neq S_{\Phi}(f)$ , with  $S_{\Phi}^+(f) \equiv S_{\Phi}(f) + S_{\Phi}(-f)$ . The asymmetric quantum part  $S_{\Phi}^-(f) \equiv S_{\Phi}(f) - S_{\Phi}(-f)$  is a measure of the environmental density of states. In thermal equilibrium, the two spectra are related through the fluctuation-dissipation theorem,  $S_{\Phi}^+(f) = \coth(hf/2k_B T) S_{\Phi}^-(f)$  [22]. In the classical regime  $f \ll 2k_B T/h$ ,  $S_{\Phi}^+$  dominates and  $S_{\Phi}^-$  is negligible unless one is sensitive to weak dissipation. Conversely, in the quantum limit of high frequencies one has  $S_{\Phi}^+ \approx S_{\Phi}^-$ , meaning a single spectrum suffices unless one is sensitive to small levels of thermal noise. But when  $f \sim k_B T/h$  or if there is non-equilibrium noise, a

single spectrum no longer characterizes the environment. Solid-state qubits are uniquely well-suited to measure environmental quantum noise due to their strong environmental coupling and faithful individual qubit readout [23, 24]. There is evidence that  $1/f$  noise in superconducting qubits contributes to relaxation in the quantum regime [15, 21], but there has been no frequency-resolved experimental distinction between  $S_{\Phi}^+$  and  $S_{\Phi}^-$  or between equilibrium and non-equilibrium noise. Furthermore, the transition from classical to quantum flux noise has yet to be observed or understood.

Experimentally, obtaining  $S_{\Phi}^-(f)$  in the classical or crossover regime is challenging, requiring high fidelity readout of the qubit population over a range of qubit frequency  $f_{10} \lesssim 2k_B T/h$ , outside typical qubit operating conditions. In this Letter, we implement a tunable gap flux qubit with a measurement scheme allowing us to study this physics. We extract the full two-sided noise spectrum over a range of  $f$  containing  $2k_B T/h \sim 1$  GHz. We observe a classical-quantum crossover, which we find to coincide with a transition from  $1/f$  to quasi-ohmic dissipation. Remarkably, we find that  $S_{\Phi}^+(f) \propto 1/f$  at 1 GHz, with a magnitude close to that extrapolated from the  $1/f$  noise below 1 Hz. The level of  $1/f$  noise at high and low frequencies changes similarly between samples [25], providing evidence they may originate from the same physical source. Below the crossover we find that the environment is close to thermal equilibrium. We measure the  $T$ -dependence of  $S_{\Phi}^{\pm}(f)$ , and discover a paramagnetic  $1/T$  scaling in  $S_{\Phi}^-$ . Finally, we show that the small  $S_{\Phi}^-$  in the classical regime has an important effect by predicting the reorganization energy during incoherent tunneling between flux qubit wells [13], a crucial quantity for modeling quantum annealers.

The coplanar waveguide (CPW)-based “fluxmon”

qubit was designed with a long loop and appreciable persistent current to allow strong coupling to many qubits at once. This also makes it a sensitive tool to study flux noise. As shown in Fig. 1(a), the fluxmon consists of a CPW shorted on one end and shunted with a DC SQUID on the other. The CPW has inductance and capacitance per unit length  $\mathcal{L}$  and  $\mathcal{C}$ , with length  $\ell$  such that at frequencies below its  $\lambda/4$  resonance, it acts as a lumped-element parallel  $L = \mathcal{L}\ell \approx 600$  pH and  $C = \mathcal{C}\ell/3 \approx 100$  fF. The high-quality CPW capacitance dominates over the junction capacitance, minimizing dielectric loss, a shared feature with the C-shunted flux qubit [21]. The linear CPW inductance replaces the need for additional large junctions, and makes the potential intrinsically one-dimensional. Shunting the CPW with a DC SQUID adds a tunable nonlinear term, allowing the potential to be varied from a harmonic single well to a conventional flux qubit double-well [45]. The potential's "tilt" is tuned by an external flux bias  $\Phi_t^x$  through the CPW, while the barrier height is tuned via the DC SQUID external flux  $\Phi_{\text{ba}}^x$ , yielding a tunable Josephson term parameterized by  $\beta = (2\pi/\Phi_0)^2 E_J L = \beta_{\text{max}} \cos(\pi\Phi_{\text{ba}}^x/\Phi_0)$ , where  $\beta_{\text{max}} \approx 2.5$ . Grounds are connected throughout the circuit with Al airbridges [46] to control linear crosstalk and coupling to spurious modes.

We implement a variation of dispersive readout inspired by phase qubits [47, 48]. After performing qubit state manipulations with microwave pulses in the single-well regime, we adiabatically project the qubit energy states into the stable left and right wells of a double-well potential with a raised barrier, as illustrated in Fig. 1(b). A large tilt is then applied to induce different well frequencies that are detected through a dispersively coupled readout resonator, yielding a single-shot separation fidelity of  $> 99.9\%$  and a  $|1\rangle$  state fidelity of  $\sim 97\%$  limited by energy decay during the projection.

At zero tilt bias, the potential energy function is symmetric, meaning the energy eigenstates  $|0\rangle$  and  $|1\rangle$  have even and odd parity. Using this parity basis in the two-level approximation, the qubit Hamiltonian can be written as  $\hat{H} = -\frac{1}{2}[\Delta(\Phi_{\text{ba}}^x)\sigma_z + \varepsilon(\Phi_t^x)\sigma_x]$ , where the gap  $\Delta/h$  is  $f_{10}$  at zero tilt, and  $\varepsilon = 2I_p\Phi_t^x$ . Here,  $I_p \equiv \frac{1}{L}\langle 0|\hat{\Phi}|1\rangle \sim 0.5 \mu\text{A}$  is the "persistent current." At zero tilt, flux noise in the main qubit loop (i.e., in  $\varepsilon$ ) at  $f_{10}$  induces incoherent transitions between energy eigenstates according to Fermi's golden rule [49]:  $\Gamma_{\downarrow/\uparrow} = \frac{1}{\hbar^2} \frac{1}{L^2} |\langle 0|\hat{\Phi}|1\rangle|^2 S_{\Phi}(\pm f_{10})$ . This implies a two-rate equation where the qubit relaxes to a steady state population  $p_{\text{stray}} = \Gamma_{\uparrow}/(\Gamma_{\downarrow} + \Gamma_{\uparrow})$  at a rate  $1/T_1 = \Gamma_{\downarrow} + \Gamma_{\uparrow}$ . From  $T_1$  and  $p_{\text{stray}}$  we extract both  $S_{\Phi}^+$  and  $S_{\Phi}^-$ :

$$S_{\Phi}^+(f_{10}) = \frac{\hbar^2 L^2}{T_1 |\langle 0|\hat{\Phi}|1\rangle|^2}, \quad (1)$$

$$S_{\Phi}^-(f_{10}) = [1 - 2p_{\text{stray}}(f_{10})]S_{\Phi}^+(f_{10}). \quad (2)$$

We measure  $T_1$  and  $p_{\text{stray}}$  vs.  $f_{10}$  at zero tilt bias

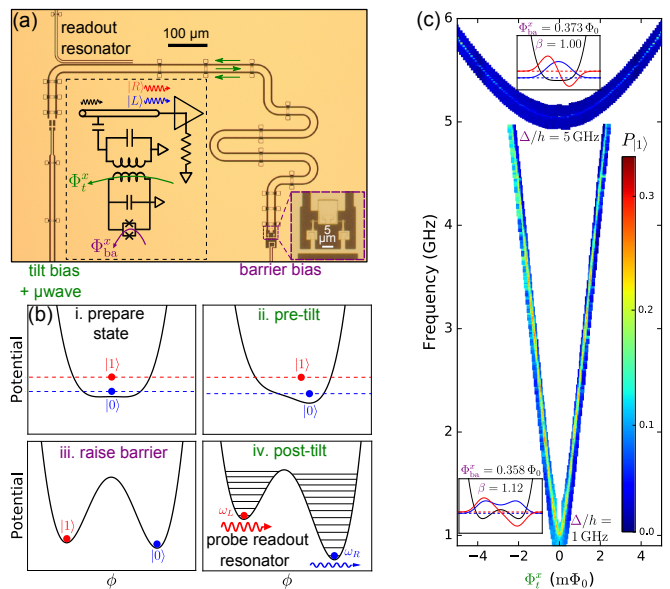


Figure 1. (color online) (a) Optical micrograph of Al/sapphire fluxmon qubit and bias lines, inductively coupled to a CPW readout resonator. The main qubit loop and bias utilize a gradiometric CPW current (arrows). (b) Four stages of measurement, involving double-well projection followed by dispersive readout. (c) Qubit spectroscopy versus frequency and  $\Phi_t^x$  for two values of  $\Delta(\Phi_{\text{ba}}^x)$ .

by varying the barrier bias, and use the data to extract  $S_{\Phi}^{\pm}(f)$  after numerically computing  $\langle 0|\hat{\Phi}|1\rangle$ . The ability to tune  $\Delta$  as in Fig. 1(c) is crucial, as it allows us to vary  $f_{10}$  while remaining at zero tilt so as to be sensitive only to transverse noise in  $\varepsilon$ . It also allows measurement over a wide frequency range within a valid two-level approximation. We use the method of swap spectroscopy [50] [Fig. 2(a) inset]: first, with  $f_{10} \approx 5$  GHz ( $\beta \approx 1$ ), the qubit is excited using a  $\pi$ -pulse, and then a barrier pulse detunes  $f_{10}$  to a different frequency. The detuning pulse is adiabatic yet much shorter than  $T_1$ . During the barrier pulse, a compensating tilt bias pulse is applied to correct for crosstalk, keeping the qubit at zero tilt. We wait for a variable time  $t$  at the detuned bias point, before tuning back to the original bias and performing readout. After measuring  $p_{|1\rangle}(t)$ , we extract  $T_1$  and  $p_{\text{stray}}$  by fitting to  $p_{|1\rangle}(t) = p_0 \exp(-t/T_1) + p_{\text{stray}}$ . A typical dataset for  $T_1$  and  $p_{\text{stray}}$  vs.  $\Delta/h$  is shown in Fig. 2 (a) and (b).

A typical dataset converted to spectral densities [Eqs. (1) and (2)] is shown in Fig. 2(c). In addition, the extracted effective temperature  $T_{\text{eff}}$  is plotted in Fig. 2(d), where  $\exp(-hf_{10}/k_B T_{\text{eff}}) \equiv \Gamma_{\uparrow}/\Gamma_{\downarrow}$ . We observe several interesting features. First, below  $\sim 1$  GHz,  $S_{\Phi}^+(f)$  follows a  $1/f^\alpha$  law, with  $\alpha \approx 1$ . Remarkably, in Fig. 2(e) we find that extrapolating this power law to frequencies below 1 Hz predicts the magnitude of the quasistatic  $1/f$  noise [25] surprisingly closely. In thermal equilibrium,  $S_{\Phi}^-(f)$  should scale as  $f^{1-\alpha}$  at low frequencies, meaning a constant  $S_{\Phi}^-(f)$  for  $1/f$  noise, which is roughly what we observe. At frequencies below the classical-quantum

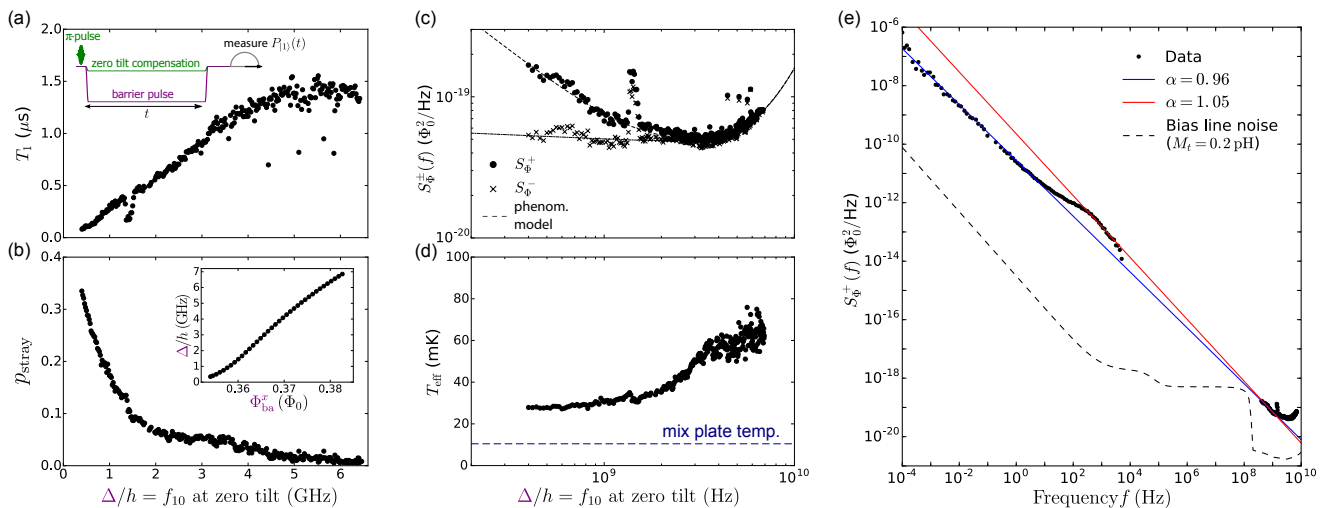


Figure 2. (a)  $T_1$  versus  $f_{10}$  at zero tilt measured with swap spectroscopy. Inset illustrates the pulse sequence. (b)  $p_{\text{stray}}$  versus  $f_{10}$  at zero tilt. Inset:  $f_{10}$  at zero tilt versus barrier bias. (c)  $S_{\Phi}^{\pm}(f)$  extracted from (a) and (b) and numerical evaluation of  $\langle 0|\hat{\Phi}|1\rangle$ . (d) Effective temperature  $T_{\text{eff}}$  of the data in (b). (e) Low-frequency quasistatic flux noise [25] together with  $S_{\Phi}^{\pm}(f)$  from (c) on the same axes.

crossover, the noise appears to be described by a single  $T_{\text{eff}} \approx 30$  mK, suggesting thermal equilibrium of the low-frequency environment, but with  $T > T_{\text{fridge}}$  [Fig. 2(d)]. We believe the peak in dissipation at 1.4 GHz may be due to coupling to the hyperfine transition of weakly bound hydrogen atoms on the qubit surface [25, 51].

Secondly, we find that the classical-quantum crossover is accompanied by a transition from  $1/f^\alpha$  to super-ohmic dissipation, meaning noise for which  $S_{\Phi}^{\pm}(f) \approx S_{\Phi}^{-}(f) \propto f^\gamma$  with  $\gamma \geq 1$ . If we fit to the phenomenological thermodynamic model  $S_{\Phi}(\omega) = A\omega/|\omega|^\alpha [1 + \coth(\hbar\omega/[2k_B T_A])] + B\omega|\omega|^{\gamma-1} [1 + \coth(\hbar\omega/[2k_B T_B])]$ , then  $\alpha = 1.05$  and  $\gamma$  between 2.5 and 3 fits our data best. Purcell decay is negligible. We note that  $\gamma = 3$  gives a frequency dependence for  $T_1$  that is indistinguishable from ohmic charge noise ( $S_Q^- \propto \omega$ ), the high-frequency model used in Ref. [21]. Dielectric loss [52] would give  $\gamma = 2$ , but based on similarly fabricated Xmon qubits and airbridges we estimate a limit of  $T_1 \sim 20 \mu\text{s}$  at 5 GHz. Allowing for a finite high-frequency cutoff for the  $1/f^\alpha$  noise could yield a different best-fit  $\gamma \approx 1.5$  [25]. If we instead simply ignore the  $1/f$  part and only fit the data above  $\sim 3.5$  GHz, an ohmic flux noise model with  $\gamma \approx 1$  describes the data reasonably well, with the net dissipation represented by a frequency-independent parallel resistance  $R \approx 20 \text{ M}\Omega$ . Dissipation from the tilt flux bias line would similarly have  $\gamma = 1$ , but with  $T_1 \approx 40 \mu\text{s}$ . Since the observed level of dissipation is not seen in the Xmon transmon qubit [53], which is comprised of a similar capacitance and Josephson inductance (albeit with a critical current density 10 times smaller) but negligible geometric inductance, we hypothesize that the quasi-ohmic noise is magnetic in nature. The presence of unexplained ohmic dissipation ( $\gamma = 1$ ) was seen in microstrip-based flux qubits [54], but with a much stronger magni-

tude ( $R \approx 20 \text{ k}\Omega$ ). Given that the extracted  $\gamma$  depends on whether the  $1/f$  noise is included in the model, it could be that this earlier result was the combined effect of  $1/f$  and super-ohmic dissipation. We note that at high frequencies,  $T_{\text{eff}}$  ranges from 50 – 80 mK, meaning a higher  $T$  for the quasi-ohmic bath and/or the presence of non-equilibrium noise, making it difficult to model.

We investigate the nature of the  $1/f$  noise further by looking at its temperature dependence. The temperature-independence of the classical low-frequency noise at millikelvin temperatures and the  $1/T$  dependence of the static susceptibility in SQUIDs are evidence of a paramagnetic origin [6] for the noise. Here, we uncover dynamical evidence for this conclusion. As shown in Fig. 3, we find that  $S_{\Phi}^{-}$  displays an approximately  $1/T$  dependence below the classical-quantum crossover point, which through the fluctuation-dissipation theorem implies that  $\chi''(\omega)$ , the imaginary (absorptive) part of the environment's dynamic susceptibility  $\chi(\omega) = \chi'(\omega) + i\chi''(\omega)$ , has a paramagnetic  $1/T$  scaling (see [25]). In comparison,  $S_{\Phi}^{+}$  displays only a very slight temperature dependence, consistent with the fact that we see no measurable temperature dependence in the quasistatic flux noise ( $f < 10 \text{ kHz}$ ) [25]. In the inset to Fig. 3 we explicitly plot  $1/S^{-}(500 \text{ MHz})$  versus  $T_{\text{eff}}$ , implying that  $\chi''(\omega, T) \propto 1/(T+T_0)$ , with  $T_0 \approx 10 \text{ mK}$ . This functional form might be taken as evidence for paramagnetic spins that would behave antiferromagnetically at lower temperatures. We also note that a model with a temperature-dependent high-frequency cutoff of a few  $k_B T_{\text{eff}}/h$  (consistent with spin-phonon or spin-spin interactions) fits the crossover region vs.  $f$  and  $T$  somewhat better than one with a fixed or infinite cutoff (see [25]).

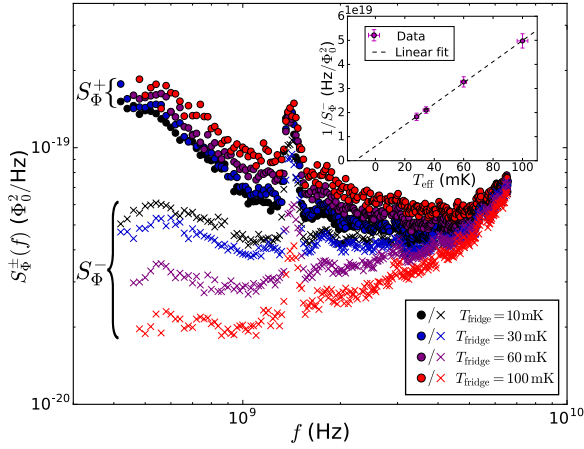


Figure 3. Temperature dependence of  $S_{\Phi}^{\pm}$ .  $S_{\Phi}^{-}(f = 500 \text{ MHz})$  shows a  $1/(T_{\text{eff}} + T_0)$  dependence, as explicitly plotted in the inset.

Finally, we show that the measured  $S_{\Phi}^{-}$  extends deep into the classical regime by performing an experiment closely tied to quantum annealing. We look at the effect of dissipation on incoherent macroscopic resonant tunneling (MRT) between the lowest states of the left and right flux qubit wells. In the regime of large  $\beta$ , the tunnel coupling  $\Delta/h$  is much smaller than the linewidth of the energy levels, meaning that quantum tunneling will be incoherent. For the level of damping and dephasing in our system, at temperatures below  $T_{\text{cr}} \approx 200 \text{ mK}$  the escape rate from one well to the other near resonance should be dominated by quantum tunneling [12, 55–57]. Rewriting the result of [12], the tunneling rate as a function of tilt bias energy  $\varepsilon$  is predicted to be

$$\Gamma_{L \rightarrow R}(\varepsilon) = \frac{\Delta^2}{4\hbar^2} \int_0^{\infty} dt e^{I_A(t)} \cos[\varepsilon t/\hbar - I_B(t)], \quad (3)$$

where  $I_A(t) = \int_{f_l}^{f_h} df \frac{(2I_p)^2}{(hf)^2} S_{\Phi}^{+}(f) \cos(2\pi ft)$ ,  $I_B(t) = \int_{f_l}^{f_h} df \frac{(2I_p)^2}{(hf)^2} S_{\Phi}^{-}(f) \sin(2\pi ft)$ , and  $f_l$  and  $f_h$  are appropriate low and high frequency cutoffs. Assuming the integrated noise is dominated by frequencies smaller than the resonant tunneling linewidth  $W/h$ , then near its peak Eq. (3) can be approximated as  $\Gamma(\varepsilon) = \sqrt{\frac{\pi}{8}} \frac{\Delta^2}{\hbar W} \exp\left[-\frac{(\varepsilon - \varepsilon_p)^2}{2W^2}\right]$ , where  $W^2 = 4I_p^2 \int_{f_l}^{f_h} df S_{\Phi}^{+}(f)$  and  $\varepsilon_p = 4I_p^2 \int_{f_l}^{f_h} df S_{\Phi}^{-}(f)/(hf)$  [12]. It is therefore possible to observe the integrated effect of  $S_{\Phi}^{-}$  in the deep classical regime by looking at the offset  $\varepsilon_p$  for the maximum tunneling rate [13], which physically corresponds to the reorganization energy of the environment that must be absorbed upon tunneling.

We measure  $\Gamma(\varepsilon)$  using the pulse sequence in Fig. 4(a). We prepare either the left or right well ground state with a high barrier, and as a function of tilt bias lower the barrier to  $\beta \approx 1.5$  ( $\Delta/h \approx 1 \text{ MHz}$ ) and measure the incoherent tunneling rate to the other well. A typical dataset is shown in Fig. 4(b). Fitting the tunneling

peaks to Gaussians, over multiple datasets we extract  $\varepsilon_p/(2I_p) = 7 \pm 3 \mu\Phi_0$  and  $W/(2I_p) = 80 \pm 20 \mu\Phi_0$ . Above base temperature  $W$  is not changed within the margin of error, but  $\varepsilon_p$  becomes too small to reliably measure.

We can compare  $W$  and  $\varepsilon_p$  to that expected from directly integrating  $S_{\Phi}^{\pm}(f)$ , interpolating a  $1/f$  power law between the noise measured at low and high frequencies [Fig. 2(e)]. Including the ohmic noise leaves the tunneling rate virtually unaffected near the peak even when integrating (3) up to  $f_h = 10 \text{ GHz}$ , the oscillation frequency of the inverted potential barrier, the natural high frequency cutoff [25, 40, 42]. The natural low-frequency cutoff for  $W$  and  $\varepsilon_p$  is the peak tunneling rate itself,  $\sim 10^3 \text{ Hz}$ . However, there is additional broadening of  $W$  due to quasistatic noise averaged over experimental repetitions, which amounts to extending the low frequency cutoff for  $W$  down to the inverse total data acquisition time [25]. Using these cutoffs we predict  $W/(2I_p) \approx 50 \mu\Phi_0$  and  $\varepsilon_p/(2I_p) \approx 4 \mu\Phi_0$ , within a factor of two of the measured values. For low-frequency noise in thermal equilibrium, one would expect  $T = W^2/(2k_B\varepsilon_p)$  [13]. Plugging in our measured  $W$  and  $\varepsilon_p$  yields  $T_{\text{eff}} \approx 60 \text{ mK}$ , higher than the  $30 \text{ mK}$  deduced in Fig. 2(d). However, this may be explained by the extra broadening of  $W$  from quasistatic noise. Subtracting out our estimation of this contribution yields instead  $20 \text{ mK}$ .

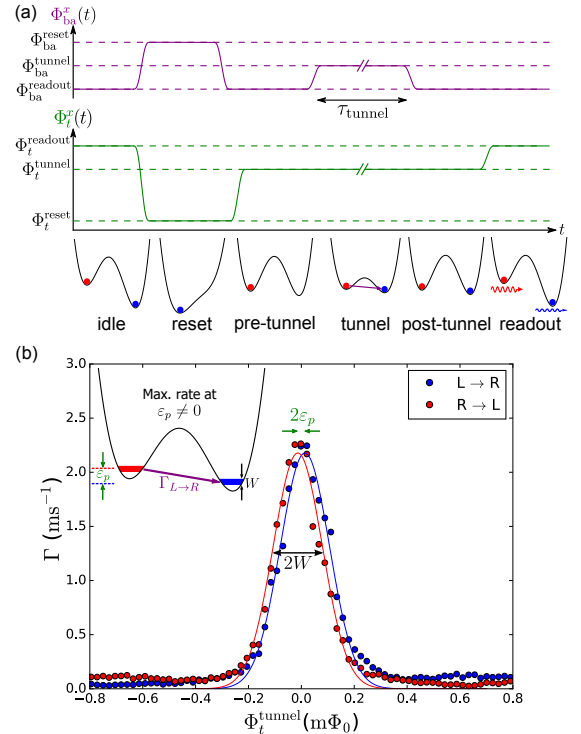


Figure 4. (a) Pulse sequence for the MRT experiment. (b) MRT data with  $\Delta/h \approx 0.5 \text{ MHz}$ , showing a small offset in the tilt bias that maximizes tunneling, consistent with the measured  $S_{\Phi}^{-}$ .

In conclusion, we have used the fluxmon to measure

flux noise over a range of frequencies about  $2k_B T/h$ , separately extracting the symmetric and antisymmetric components  $S_{\Phi}^{\pm}(f)$  and observing the classical-quantum crossover. We find that  $S_{\Phi}^{-}$  displays a paramagnetic temperature dependence below the crossover, and that  $S_{\Phi}^{+}$  follows a  $1/f$  power law whose magnitude is consistent with that of the  $1/f$  flux noise near 1 Hz. The fact that the noise spectrum has a  $1/f$  shape near the crossover indicates that the underlying magnetic fluctuators have a distribution of relaxation times that extends to at least 1 GHz, possibly hinting towards spin clustering as opposed to spin diffusion [25, 58, 59], which would also be consistent with the correlated low-frequency inductance fluctuations observed in SQUIDs that were postulated to arise from fluctuations in spin cluster relaxation times [60]. Recent evidence [9] that adsorbed molecular  $O_2$  (spin-1) may play a dominant role in flux noise could also support this conclusion, as spin-orbit induced magnetic anisotropy could break conservation of total spin and allow clusters to locally transfer energy and angular momentum to the lattice. Finally, we showed that the measured noise and dissipation can approximately predict incoherent quantum tunneling rates between flux qubit wells, which has direct implications for quantum annealing applications.

We thank Sergio Boixo, Robert McDermott, Fedir Vasko, Mostafa Khezri, Fei Yan, and Sebastian de Graaf for insightful discussions. This work was supported by Google. C. Q. and Z. C. acknowledge support from the National Science Foundation Graduate Research Fellowship under Grant No. DGE-1144085. A. P. acknowledges support from the Air Force Research Laboratory (AFRL) Information Directorate under grant F4HBKC4162G001. Devices were made at the UC Santa Barbara Nanofabrication Facility, a part of the NSF-funded National Nanotechnology Infrastructure Network.

- 
- [1] J. Clarke, W. M. Goubau, and M. B. Ketchen, *Journal of Low Temperature Physics* **25**, 99 (1976).
- [2] R. H. Koch, J. Clarke, W. M. Goubau, J. M. Martinis, C. M. Pegrum, and D. J. van Harlingen, *Journal of Low Temperature Physics* **51**, 207 (1983).
- [3] F. C. Wellstood, C. Urbina, and J. Clarke, *Applied Physics Letters* **50**, 772 (1987).
- [4] F. Yoshihara, K. Harrabi, A. O. Niskanen, Y. Nakamura, and J. S. Tsai, *Phys. Rev. Lett.* **97**, 167001 (2006).
- [5] R. C. Bialczak, R. McDermott, M. Ansmann, M. Hofheinz, N. Katz, E. Lucero, M. Neeley, A. D. O’Connell, H. Wang, A. N. Cleland, and J. M. Martinis, *Phys. Rev. Lett.* **99**, 187006 (2007).
- [6] S. Sendelbach, D. Hover, A. Kittel, M. Mück, J. M. Martinis, and R. McDermott, *Phys. Rev. Lett.* **100**, 227006 (2008).
- [7] T. Lanting, A. J. Berkley, B. Bumble, P. Bunyk, A. Fung, J. Johansson, A. Kaul, A. Kleinsasser, E. Ladizinsky, F. Maibaum, R. Harris, M. W. Johnson, E. Tolkacheva, and M. H. S. Amin, *Phys. Rev. B* **79**, 060509 (2009).
- [8] S. M. Anton, J. S. Birenbaum, S. R. O’Kelley, V. Bolkhovskiy, D. A. Braje, G. Fitch, M. Neeley, G. C. Hilton, H.-M. Cho, K. D. Irwin, F. C. Wellstood, W. D. Oliver, A. Shnirman, and J. Clarke, *Phys. Rev. Lett.* **110**, 147002 (2013).
- [9] P. Kumar, S. Sendelbach, M. A. Beck, J. W. Freeland, Z. Wang, H. Wang, C. C. Yu, R. Q. Wu, D. P. Pappas, and R. McDermott, *Phys. Rev. Applied* **6**, 041001 (2016).
- [10] A. J. Leggett, *Phys. Rev. B* **30**, 1208 (1984).
- [11] D. Esteve, M. H. Devoret, and J. M. Martinis, *Phys. Rev. B* **34**, 158 (1986).
- [12] M. H. S. Amin and D. V. Averin, *Phys. Rev. Lett.* **100**, 197001 (2008).
- [13] R. Harris, M. W. Johnson, S. Han, A. J. Berkley, J. Johansson, P. Bunyk, E. Ladizinsky, S. Govorkov, M. C. Thom, S. Uchaikin, B. Bumble, A. Fung, A. Kaul, A. Kleinsasser, M. H. S. Amin, and D. V. Averin, *Phys. Rev. Lett.* **101**, 117003 (2008).
- [14] S. Boixo, V. N. Smelyanskiy, A. Shabani, S. V. Isakov, M. Dykman, V. S. Denchev, M. H. Amin, A. Y. Smirnov, M. Mohseni, and H. Neven, *Nature communications* **7** (2016).
- [15] J. Bylander, S. Gustavsson, F. Yan, F. Yoshihara, K. Harrabi, G. Fitch, D. G. Cory, Y. Nakamura, J.-S. Tsai, and W. D. Oliver, *Nature Physics* **7**, 565 (2011).
- [16] D. Sank, R. Barends, R. C. Bialczak, Y. Chen, J. Kelly, M. Lenander, E. Lucero, M. Mariantoni, A. Megrant, M. Neeley, P. J. J. O’Malley, A. Vainsencher, H. Wang, J. Wenner, T. C. White, T. Yamamoto, Y. Yin, A. N. Cleland, and J. M. Martinis, *Phys. Rev. Lett.* **109**, 067001 (2012).
- [17] F. Yan, J. Bylander, S. Gustavsson, F. Yoshihara, K. Harrabi, D. G. Cory, T. P. Orlando, Y. Nakamura, J.-S. Tsai, and W. D. Oliver, *Phys. Rev. B* **85**, 174521 (2012).
- [18] D. H. Slichter, R. Vijay, S. J. Weber, S. Boutin, M. Boissonneault, J. M. Gambetta, A. Blais, and I. Siddiqi, *Phys. Rev. Lett.* **109**, 153601 (2012).
- [19] F. Yan, S. Gustavsson, J. Bylander, X. Jin, F. Yoshihara, D. G. Cory, Y. Nakamura, T. P. Orlando, and W. D. Oliver, *Nature communications* **4** (2013).
- [20] F. Yoshihara, Y. Nakamura, F. Yan, S. Gustavsson, J. Bylander, W. D. Oliver, and J.-S. Tsai, *Phys. Rev. B* **89**, 020503 (2014).
- [21] F. Yan, S. Gustavsson, A. Kamal, J. Birenbaum, A. P. Sears, D. Hover, T. J. Gudmundsen, D. Rosenberg, G. Samach, S. Weber, J. L. Yoder, T. P. Orlando, J. Clarke, A. J. Kerman, and W. D. Oliver, *arXiv preprint arXiv:1508.06299* (2016).
- [22] M. H. Devoret, Les Houches, Session LXIII **7** (1997).
- [23] R. Deblock, E. Onac, L. Gurevich, and L. P. Kouwenhoven, *Science* **301**, 203 (2003).
- [24] O. Astafiev, Y. A. Pashkin, Y. Nakamura, T. Yamamoto, and J. S. Tsai, *Phys. Rev. Lett.* **93**, 267007 (2004).
- [25] See Supplemental Material [url], which includes Refs. [26-44].
- [26] Y.-H. Lu and H.-T. Chen, *Phys. Chem. Chem. Phys.* **17**, 6834 (2015).
- [27] T. Van Duzer and C. W. Turner, *Principles of superconductive devices and circuits* (1981).
- [28] I. Tupitsyn and S. Kotochigova, *J. Res. Natl. Inst. Stand. Technol.* **103**, 205 (1998).

- [29] J. Koch, T. M. Yu, J. Gambetta, A. A. Houck, D. I. Schuster, J. Majer, A. Blais, M. H. Devoret, S. M. Girvin, and R. J. Schoelkopf, *Phys. Rev. A* **76**, 042319 (2007).
- [30] G. Catelani, R. J. Schoelkopf, M. H. Devoret, and L. I. Glazman, *Phys. Rev. B* **84**, 064517 (2011).
- [31] I. M. Pop, K. Geerlings, G. Catelani, R. J. Schoelkopf, L. I. Glazman, and M. H. Devoret, *Nature* **508**, 369 (2014).
- [32] J. M. Martinis, M. Ansmann, and J. Aumentado, *Phys. Rev. Lett.* **103**, 097002 (2009).
- [33] M. Lenander, H. Wang, R. C. Bialczak, E. Lucero, M. Mariantoni, M. Neeley, A. D. O’Connell, D. Sank, M. Weides, J. Wenner, T. Yamamoto, Y. Yin, J. Zhao, A. N. Cleland, and J. M. Martinis, *Phys. Rev. B* **84**, 024501 (2011).
- [34] J. Wenner, Y. Yin, E. Lucero, R. Barends, Y. Chen, B. Chiaro, J. Kelly, M. Lenander, M. Mariantoni, A. Megrant, C. Neill, P. J. J. O’Malley, D. Sank, A. Vainsencher, H. Wang, T. C. White, A. N. Cleland, and J. M. Martinis, *Phys. Rev. Lett.* **110**, 150502 (2013).
- [35] D. Ristè, C. Bultink, M. Tiggelman, R. Schouten, K. Lehnert, and L. DiCarlo, *Nat. Commun.* **4**, 1913 (2013).
- [36] U. Vool, I. M. Pop, K. Sliwa, B. Abdo, C. Wang, T. Brecht, Y. Y. Gao, S. Shankar, M. Hatridge, G. Catelani, M. Mirrahimi, L. Frunzio, R. J. Schoelkopf, L. I. Glazman, and M. H. Devoret, *Phys. Rev. Lett.* **113**, 247001 (2014).
- [37] C. Wang, Y. Y. Gao, I. M. Pop, U. Vool, C. Axline, T. Brecht, R. W. Heeres, L. Frunzio, M. H. Devoret, G. Catelani, *et al.*, *Nature communications* **5** (2014).
- [38] X. Y. Jin, A. Kamal, A. P. Sears, T. Gudmundsen, D. Hover, J. Miloshi, R. Slattery, F. Yan, J. Yoder, T. P. Orlando, S. Gustavsson, and W. D. Oliver, *Phys. Rev. Lett.* **114**, 240501 (2015).
- [39] R. Barends, J. Wenner, M. Lenander, Y. Chen, R. C. Bialczak, J. Kelly, E. Lucero, P. O’Malley, M. Mariantoni, D. Sank, H. Wang, T. C. White, Y. Yin, J. Zhao, A. N. Cleland, J. M. Martinis, and J. J. A. Baselmans, *Appl. Phys. Lett.* **99**, 113507 (2011).
- [40] M. Büttiker and R. Landauer, *Phys. Rev. Lett.* **49**, 1739 (1982).
- [41] J. M. Martinis, M. H. Devoret, D. Esteve, and C. Urbina, *Physica B: Condensed Matter* **152**, 159 (1988).
- [42] D. Esteve, J. M. Martinis, C. Urbina, E. Turlot, M. H. Devoret, H. Grabert, and S. Linkwitz, *Physica Scripta* **1989**, 121 (1989).
- [43] T. Lanting, M. H. Amin, A. J. Berkley, C. Rich, S.-F. Chen, S. LaForest, and R. de Sousa, *Phys. Rev. B* **89**, 014503 (2014).
- [44] A. G. Petukhov, V. N. Smelyanskiy and J. M. Martinis (in preparation).
- [45] J. Mooij, T. Orlando, L. Levitov, L. Tian, C. H. Van der Wal, and S. Lloyd, *Science* **285**, 1036 (1999).
- [46] Z. Chen, A. Megrant, J. Kelly, R. Barends, J. Bochmann, Y. Chen, B. Chiaro, A. Dunsworth, E. Jeffrey, J. Y. Mutus, P. J. J. O’Malley, C. Neill, P. Roushan, D. Sank, A. Vainsencher, J. Wenner, T. C. White, A. N. Cleland, and J. M. Martinis, *Applied Physics Letters* **104**, 052602 (2014), 10.1063/1.4863745.
- [47] M. Steffen, S. Kumar, D. DiVincenzo, G. Keefe, M. Ketchen, M. B. Rothwell, and J. Rozen, *Applied Physics Letters* **96**, 102506 (2010), 10.1063/1.3354089.
- [48] Y. Chen, D. Sank, P. O’Malley, T. White, R. Barends, B. Chiaro, J. Kelly, E. Lucero, M. Mariantoni, A. Megrant, C. Neill, A. Vainsencher, J. Wenner, Y. Yin, A. N. Cleland, and J. M. Martinis, *Applied Physics Letters* **101**, 182601 (2012), 10.1063/1.4764940.
- [49] R. J. Schoelkopf, A. A. Clerk, S. M. Girvin, K. W. Lehnert, and M. H. Devoret, *Proc. SPIE* **5115**, 356 (2003).
- [50] M. Mariantoni, H. Wang, R. C. Bialczak, M. Lenander, E. Lucero, M. Neeley, A. O’Connell, D. Sank, M. Weides, J. Wenner, *et al.*, *Nature Physics* **7**, 287 (2011).
- [51] S. E. de Graaf, A. A. Adamy, T. Lindström, D. Erts, S. E. Kubatkin, A. Y. Tzalenchuk, and A. V. Danilov, *arXiv preprint arXiv:1609.04562* (2016).
- [52] J. M. Martinis, K. B. Cooper, R. McDermott, M. Steffen, M. Ansmann, K. D. Osborn, K. Cicak, S. Oh, D. P. Pappas, R. W. Simmonds, and C. C. Yu, *Phys. Rev. Lett.* **95**, 210503 (2005).
- [53] R. Barends, J. Kelly, A. Megrant, D. Sank, E. Jeffrey, Y. Chen, Y. Yin, B. Chiaro, J. Mutus, C. Neill, P. O’Malley, P. Roushan, J. Wenner, T. C. White, A. N. Cleland, and J. M. Martinis, *Phys. Rev. Lett.* **111**, 080502 (2013).
- [54] T. Lanting, M. H. S. Amin, M. W. Johnson, F. Altomare, A. J. Berkley, S. Gildert, R. Harris, J. Johansson, P. Bunyk, E. Ladizinsky, E. Tolkacheva, and D. V. Averin, *Phys. Rev. B* **83**, 180502 (2011).
- [55] M. Büttiker, E. P. Harris, and R. Landauer, *Phys. Rev. B* **28**, 1268 (1983).
- [56] M. H. Devoret, J. M. Martinis, and J. Clarke, *Phys. Rev. Lett.* **55**, 1908 (1985).
- [57] J. M. Martinis, M. H. Devoret, and J. Clarke, *Phys. Rev. B* **35**, 4682 (1987).
- [58] L. Faoro and L. B. Ioffe, *Phys. Rev. Lett.* **100**, 227005 (2008).
- [59] H. Wang, C. Shi, J. Hu, S. Han, C. C. Yu, and R. Q. Wu, *Phys. Rev. Lett.* **115**, 077002 (2015).
- [60] S. Sendelbach, D. Hover, M. Mück, and R. McDermott, *Phys. Rev. Lett.* **103**, 117001 (2009).